Agricultural and Forest Meteorology 262 (2018) 354–360

Contents lists available at ScienceDirect

Agricultural and Forest Meteorology

journal homepage: www.elsevier.com/locate/agrformet

A model for leaf temperature decoupling from air temperature

Benjamin Blonder[a,b,c,*], Sean T. Michaletz[b,d,e]

[a] Environmental Change Institute, School of Geography and the Environment, University of Oxford, South Parks Road, Oxford, OX1 3QY, United Kingdom
[b] Rocky Mountain Biological Laboratory, P.O. Box 519, Crested Butte, CO, 81224, USA
[c] School of Life Sciences, Arizona State University, P.O. Box 874501, Tempe, Arizona, 85287, USA
[d] Earth and Environmental Sciences Division, Los Alamos National Laboratory, MS-J495, Los Alamos, NM, 87545, USA
[e] Department of Botany and Biodiversity Research Centre, University of British Columbia, Vancouver, British Columbia, V6T 1Z4, Canada

ARTICLE INFO

Keywords:
Leaf temperature
Stomatal regulation
Heat stress
Energy balance
Ecophysiology

ABSTRACT

Leaf temperature (T_{leaf}) influences rates of respiration, photosynthesis, and transpiration. The local slope of the relationship between T_{leaf} and T_{air}, β, describes leaf thermal responses. A range of values have been observed, with $\beta < 1$ indicating limited homeothermy where T_{leaf} increases at a lower rate than T_{air}, $\beta = 1$ indicating poikilothermy where T_{leaf} tracks T_{air}, and $\beta > 1$ indicating megathermy where T_{leaf} increasingly exceeds T_{air}. However, theory for variation in β has not been developed. Here we derive an equation for β that predicts how it varies with multiple trait and microenvironment variables. The approach also predicts how maintenance of T_{leaf} away from lethally high values may help explain regulation of stomatal conductance (g_S). The work delineates contexts in which each class of leaf thermal response is expected and develops concepts for predicting leaf responses to thermally extreme environments.

1. Introduction

Leaf temperature, T_{leaf}, partially determines several ecophysiological rates, including carbon assimilation (A) via photosynthesis and respiration (Berry and Bjorkman, 1980; Tuzet et al., 2003), and transpiration (E) via stomatal conductance (g_S), e.g. Leuning et al. (1995); Tuzet et al. (2003). T_{leaf} is also important in ecosystem and region-scale water, carbon, and energy budgets, e.g. in various dynamic global vegetation models (Best et al., 2011; Oleson et al., 2010; Sitch et al., 2003). T_{leaf} often differs from T_{air} (Michaletz et al., 2016, 2015), and this decoupling can have major influences on carbon and water fluxes. In some cases, T_{leaf} can exceed T_{air} by up to 20 °C, e.g. in the alpine (Salisbury and Spomer, 1964) and in the humid tropics (Doughty and Goulden, 2008), while in other cases, e.g. warm deserts, T_{leaf} can be below T_{air} by 15–20 °C (Smith, 1978).

The rate at which T_{leaf} changes with changes in T_{air} characterizes the thermal response of the leaf and the decoupling of the leaf from the atmosphere. This rate is a dimensionless slope defining the local rate of change in T_{leaf} with T_{air} (Huey and Slatkin, 1976):

$$\beta = T'_{leaf}[T_{air}] = \frac{\partial T_{leaf}}{\partial T_{air}} \quad (1)$$

where the prime (′) notation indicates a derivative with respect to T_{air} and the $[T_{air}]$ notation indicates a dependence on T_{air}. Identifying the factors that drive variation in β is important for understanding leaf performance across environments. The value of β may be useful for heuristic prediction of rates of photosynthesis, respiration, and transpiration in earth systems models. Additionally, the value of β may be useful for understanding biophysical thermal effects on plant ecological strategies. Maintaining or avoiding certain temperatures may be advantageous to a plant's growth, survival, or reproduction. For example, species in cold thermal environments might experience selection for high values of β to increase T_{leaf} relative to T_{air}, improving growth rates and avoiding freezing mortality, while those in warm thermal environments might experience selection for low values of β to reduce T_{leaf} relative to T_{air}, improving growth rates and avoiding high temperature mortality. These strategies could potentially be achieved via selection on traits influencing β over evolutionary time.

The classes of possible leaf thermal responses can range from limited homeothermy ($\beta < 1$) (Gates, 1964; Mahan and Upchurch, 1988) in which $T_{leaf} > T_{air}$ below a certain temperature and $T_{leaf} < T_{air}$ otherwise, poikilothermy ($\beta = 1$) in which $T_{leaf} = T_{air}$ (Ansari and Loomis, 1959; Fetcher, 1981), and megathermy ($\beta > 1$) in which T_{leaf} increasingly exceeds T_{air} as T_{air} increases (Salisbury and Spomer, 1964). All of these classes of thermal response occur in natural settings. In many cases, β is approximately constant for a species, leading to linear $T_{leaf} - T_{air}$ relationships. However in other cases curvilinear $T_{leaf} - T_{air}$ relationships are observed, indicating that the value of β may change

* Corresponding author at: School of Life Sciences, Arizona State University, P.O. Box 874501, Tempe, AZ, 85287, USA.
E-mail address: bblonder@asu.edu (B. Blonder).

https://doi.org/10.1016/j.agrformet.2018.07.012
Received 23 March 2018; Received in revised form 11 July 2018; Accepted 13 July 2018
Available online 01 August 2018
0168-1923/ © 2018 Elsevier B.V. All rights reserved.

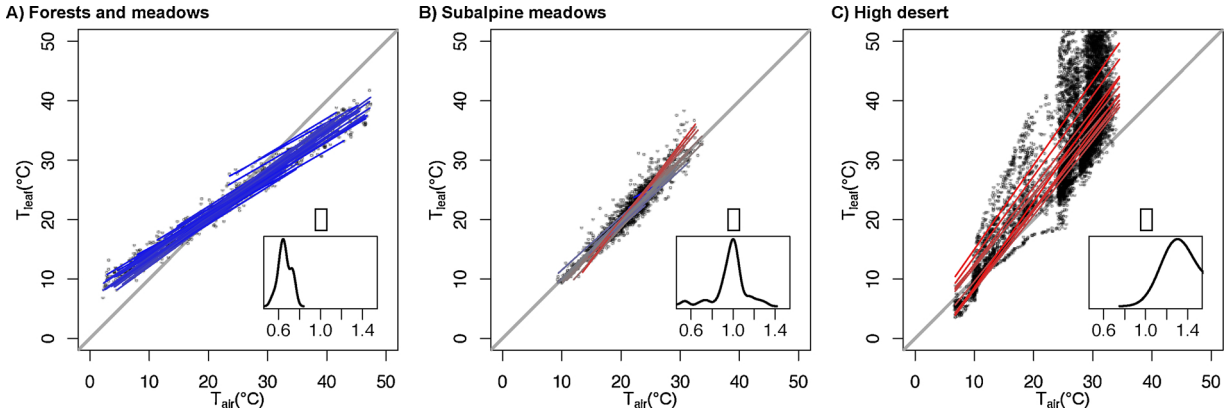


Fig. 1. Classes of leaf thermal response, defined as the slope, β, of the T_{leaf} - T_{air} relationship. Limited homeothermy ($\beta < 1$, blue lines) occurs when T_{leaf} increases more slowly than T_{air}. Poikilothermy ($\beta = 1$) (gray lines) occurs when T_{leaf} equals T_{air}. Megathermy (red lines) occurs when T_{leaf} increases more quickly than T_{air}. **A)** Data from forests and meadows (1005 observations of 15 species) show limited homeothermy. **B)** Data from subalpine meadows (2257 observations of 37 species) show poikilothermy. **C)** Data from a high desert (124,933 observations of 4 species) show megathermy. Linear regression lines through data for each leaf at different time points are colored redder if $\beta > 1$, gray if $\beta = 1$, and bluer if $\beta < 1$. Inset shows density plot of estimated β values. Thick gray line indicates the 1:1 poikilothermy expectation. Points show individual temperature measurements. (For interpretation of the references to colour in this figure legend, the reader is referred to the web version of this article).

across contexts. We present exemplar data for each class of behavior in Fig. 1, based on our original field observations of multiple co-occurring species in meadows, forests, and deserts in North America. Field methods are described in File S1 and data are provided in File S2. Additionally, in a recent global meta-analysis of leaf thermal observations (Michaletz et al., 2016), β was commonly near 3/4 independent of the value of T_{air} (i.e. limited homeothermy with no curvilinearity). However, in those data, both lower and higher values of β also occurred, indicating that there is wide variation in leaf thermal response across species and contexts. While limited homeothermy, poikilothermy, and megathermy will have different implications for plant functioning and performance, the mechanisms that determine when each class occurs have not been fully explored.

Determining how β varies in thermally extreme environments is also a priority for understanding plant performance in a changing climate. High T_{leaf} can increase rates of respiration (Heskel et al., 2016), depress rates of photosynthesis (Doughty and Goulden, 2008; Michaletz, 2018; Slot and Winter, 2017), and increase rates of cell necrosis and leaf mortality (Bilger et al., 1984). Transpiration may sometimes be a cooling strategy to improve net carbon gain, either via avoidance of mortality (i.e. loss of all future carbon gain) or via homeostasis of temperature (i.e. maintenance near the optimal temperature for photosynthesis). Some data from temperate biomes and glasshouses support this (Drake et al., 2018; Slot and Winter, 2016; Teskey et al., 2015; von Caemmerer and Evans, 2015), as do some limited tropical field data (Schulze et al., 1973; Slot and Winter, 2016). However, when hotter environments drive high transpiration demand, intrinsic limitation of g_S to a physiological maximum may drive large increases in T_{leaf}. Alternatively, maintenance of T_{leaf} below a lethal maximum may require large increases in g_S. Better understanding these tradeoffs could help improve existing theory for stomatal regulation that is focused on optimizing g_S to maximize carbon gain rather than to regulate T_{leaf}, e.g. (Medlyn et al., 2011).

There is an opportunity to obtain general insights into the factors that can influence variation in β. While direct predictions of T_{leaf} are already possible from energy balance theory (Campbell and Norman, 2012; Gates, 1980; Monteith and Unsworth, 2007; Paw U, 1987), less is known about what determines *rates of change* in T_{leaf}, i.e. β. Here we derive an exact analytical solution for β from energy balance theory. We then use this solution to predict when each class of leaf thermal response occurs, highlighting the specific environment or trait drivers underlying each scenario. We then derive additional theory for g_S, also based on energy balance theory, which highlights the strategies available to leaves in thermally extreme environments.

2. Methods

We begin with a classic result from energy balance theory following the notation of Monteith and Unsworth (2007). The energy budget of a leaf can be written as:

$$\varepsilon R_l - 2\varepsilon\sigma T_{\text{leaf}}^4 + R_s\alpha_s = 2\rho c_P\left(\frac{-T_{\text{air}} + T_{\text{leaf}}}{r_H} + \frac{ng_S(-he_s[T_{\text{air}}] + e_s[T_{\text{leaf}}])}{\gamma + \gamma g_S r_H}\right) \quad (2)$$

A derivation of this equation is available in File S3; definitions of all parameters are given in Table 1. Further analytical progress toward β by solving for T_{leaf} and applying Eq. (1) is not immediately possible, because T_{leaf} cannot be isolated as a function of T_{air}. This is because T_{leaf} appears in polynomial terms and in nonlinear e_S and r_H functions, yielding an insoluble transcendental equation. While the Penman linearization allows for an approximate solution for T_{leaf} (e.g. (Campbell and Norman, 2012; Monteith, 1965)), we advance without such approximations.

We now present an approach to obtain an exact explicit solution for β. The approach relies on implicit differentiation of Eq. (2), which eliminates the need to first solve for T_{leaf}. To begin, we assume that all parameters may vary with T_{air}, except for the physical constant σ and those that do not vary substantially across the range of T_{air} in which leaves can function (γ, ρ, c_P) or covary substantially with T_{air} over the lifespan of a leaf (n, ε, α_s). Implicit partial differentiation with respect to T_{air} of Eq. (2) yields

$$\begin{aligned}
&-8\beta\varepsilon\sigma T_{\text{leaf}}[T_{\text{air}}]^3 + \varepsilon R_l'[T_{\text{air}}] + \alpha_s R_s'[T_{\text{air}}] \\
&= 2\rho c_P\left(\frac{-1+\beta}{r_H[T_{\text{air}}]} + \frac{ng_S[T_{\text{air}}](-e_s[T_{\text{air}}]h'[T_{\text{air}}] - h[T_{\text{air}}]e_s'[T_{\text{air}}] + \beta e_s'[T_{\text{leaf}}[T_{\text{air}}]])}{\gamma + \gamma g_S[T_{\text{air}}]r_H[T_{\text{air}}]}\right. \\
&\quad + \frac{n(-h[T_{\text{air}}]e_s[T_{\text{air}}] + e_s[T_{\text{leaf}}[T_{\text{air}}]])g_S'[T_{\text{air}}]}{\gamma + \gamma g_S[T_{\text{air}}]r_H[T_{\text{air}}]} - \frac{(-T_{\text{air}} + T_{\text{leaf}}[T_{\text{air}}])r_H'[T_{\text{air}}]}{r_H[T_{\text{air}}]^2} \\
&\quad \left. - \frac{n(-h[T_{\text{air}}]e_s[T_{\text{air}}] + e_s[T_{\text{leaf}}[T_{\text{air}}]])g_S[T_{\text{air}}](\gamma r_H[T_{\text{air}}]g_S'[T_{\text{air}}] + \gamma g_S[T_{\text{air}}]r_H'[T_{\text{air}}])}{(\gamma + \gamma g_S[T_{\text{air}}]r_H[T_{\text{air}}])^2}\right)
\end{aligned} \quad (3)$$

This equation is linear in β, which means it can be algebraically rearranged to yield the solution:

Table 1
Definitions of model parameters and central values used to draw example figures.

Scale	Definition	Parameter	Units	Value
Constant	Stefan-Boltzmann constant	σ	$W\ m^{-2}\ K^{-4}$	5.67×10^{-8}
	Vapor pressure approximation constant	v_0	Pa	611.21
	Vapor pressure approximation constant	v_1	K	18.68
	Vapor pressure approximation constant	v_2	K	273.15
	Vapor pressure approximation constant	v_3	K	234.50
	Vapor pressure approximation constant	v_4	K	257.14
	Mass density of air	ρ	$g\ m^{-3}$	1225
	Psychrometer constant	γ	$Pa\ K^{-1}$	67
	Heat capacity of air	c_P	$J\ g^{-1}\ K^{-1}$	1.01
Micro-environment	Air temperature	T_{air}	K	293
	Leaf temperature	T_{leaf}	K	293
	Relative humidity	h	–	0.5
	Vapor pressure	e_S	Pa	–
	Wind speed	u	$m\ s^{-1}$	1
	Incident longwave radiation	R_l	$W\ m^{-2}$	400
	Incident shortwave radiation	R_s	$W\ m^{-2}$	800
Trait	Emissivity	ε	–	0.97
	Absorptance (shortwave)	α_s	–	0.5
	Convective resistance	r_H	$s\ m^{-1}$	100
	Stomatal conductance	g_S	$m\ s^{-1}$	0.005
	Stomatal ratio	n	–	1

$$\beta = \frac{\omega_1}{\omega_2} \tag{4}$$

where

$$\begin{aligned}\omega_1 = &-\frac{1}{\gamma r_H[T_{\text{air}}]^2(1+g_S[T_{\text{air}}]r_H[T_{\text{air}}])^2}2\rho c_P(r_H[T_{\text{air}}]((1\\ &+g_S[T_{\text{air}}]r_H[T_{\text{air}}])(\gamma+g_S[T_{\text{air}}]r_H[T_{\text{air}}](\gamma+ne_s[T_{\text{air}}]h'[T_{\text{air}}]\\ &+nh[T_{\text{air}}]e_s'[T_{\text{air}}]))+n(h[T_{\text{air}}]e_s[T_{\text{air}}]-e_s[T_{\text{leaf}}])r_H[T_{\text{air}}]g_S'[T_{\text{air}}])\\ &+(n(-h[T_{\text{air}}]e_s[T_{\text{air}}]+e_s[T_{\text{leaf}}])g_S[T_{\text{air}}]^2r_H[T_{\text{air}}]^2\\ &-\gamma T_{\text{air}}(1+g_S[T_{\text{air}}]r_H[T_{\text{air}}])^2+\gamma T_{\text{leaf}}(1+g_S[T_{\text{air}}]r_H[T_{\text{air}}])^2)r_H'[T_{\text{air}}])\\ &-\varepsilon R_l'[T_{\text{air}}]-\alpha_s R_s'[T_{\text{air}}]\end{aligned} \tag{5}$$

$$\omega_2 = 8\varepsilon\sigma T_{\text{leaf}}^3 + 2\rho c_P\left(\frac{1}{r_H[T_{\text{air}}]}+\frac{ng_S[T_{\text{air}}]e_s'[T_{\text{leaf}}]}{\gamma+\gamma g_S[T_{\text{air}}]r_H[T_{\text{air}}]}\right) \tag{6}$$

Eq. (4) can now be manipulated, simplified under limiting cases, and numerically parameterized. Additionally, computer-manipulable versions of this equation (as well as several simplified forms presented in the Results) are available in Mathematica language as File S4 and File S5, and a numerical version of Eq. (4) is available in R language as File S6.

3. Results

Conceptual insights into the drivers of β can be obtained by examining limiting cases of Eq. (4), by exploring covariance among variables, and by making numerical simulations. The exact solution for β depended on several physical constants, microenvironmental variables, and trait variables delineated in Table 1. Limiting cases (exploring the consequences of taking certain variables to zero or infinite values) provide an approach to explore the effects of biologically 'small' and 'large' values of each variable. These analyses involve starting with a minimal set of covariances between model variables and T_{air}, then adding additional covariances in order to model increasingly realistic phenomena.

3.1. Limiting cases without covariances

First, in a simple case assuming no covariance between model variables and T_{air} (except for the saturation vapor pressure of air and thus the vapor pressure deficit, which must change due to physical law), the solution for β becomes β_{const} and reduces to:

$$\beta_{const} = \frac{\rho c_P(\gamma + g_S r_H(\gamma + hne_s'[T_{\text{air}}]))}{4\gamma\varepsilon\sigma r_H(1+g_S r_H)T_{\text{leaf}}^3 + \rho c_P(\gamma + g_S r_H(\gamma + ne_s'[T_{\text{leaf}}]))} \tag{7}$$

There are two implications that arise from this simplified formulation. First, the term in the numerator is always no larger than the second term in the denominator, because h is always between 0 and 1. The first term in the denominator is strictly positive, because all parameters are non-negative. This analysis proves that under these assumptions, the value of β must always be bounded between 0 and 1. That is, when variables in the energy balance are uncorrelated with variation in T_{air}, only limited homeothermy and poikilothermy are possible. Second, β_{const} can be further simplified when stomatal conductance is zero as

$$\lim_{g_S \to 0} \beta_{const} = \frac{1}{1 + \frac{4\varepsilon\sigma}{\rho c_P} r_H T_{\text{leaf}}^3} \tag{8}$$

Thus, when transpiration is zero or small, β_{const} decreases when either r_H or T_{leaf} increases, due to nonlinearities in the relationship between radiative and convective heat transport. The overall outcome is curvilinearity in $T_{leaf} - T_{air}$ plots.

3.2. Limiting cases with covariances

Additional insights are also possible using the full solution for β where covariances between variables are possible. First, consider the limiting case of a smooth approach to no resistance to convective heat transport, i.e. $r_H = 0$ and $r_H' = 0$. In this case,

$$\lim_{(r_H, r_H') \to 0} \beta = 1 \tag{9}$$

Thus, poikilothermy is the *only* scenario possible when there is no resistance to convective heat transport, i.e. when there is full coupling between leaves and the atmosphere. Because r_H of isolated leaves often scales with the square root of the ratio of leaf size to wind speed (Monteith and Unsworth, 2007), this result also indicates that poikilothemy will occur for small leaves or high wind speeds. However, the sheltering effect of non-isolated leaves in complex canopies (Michaletz and Johnson, 2006; Smith and Carter, 1988) means that r_H is unlikely to reach zero and poikilothermy is less likely to occur.

An alternative scenario occurs when the resistance to convective heat transport becomes very large, i.e. for large leaves or low wind

speeds (though at low wind speeds free convection may prevent this resistance from becoming strictly infinite). In this case,

$$\lim_{r_H \to \infty} \beta = \frac{\varepsilon R_l'[T_{\text{air}}] + \alpha_s R_s'[T_{\text{air}}]}{8\varepsilon\sigma T_{\text{leaf}}^3} \tag{10}$$

This equation demonstrates that β decreases with increasing T_{leaf}, and increases when either R_s or R_l positively covary with T_{air}. Some positive covariance between R_l and T_{air} is likely due to heat transfer between air and ground leading to correlations between air and ground temperatures. Additionally, the numerator of Eq. (10) is potentially unbounded, with the numerator exceeding the denominator when $\varepsilon R_l'[T_{air}] + \alpha_s R_s'[T_{\text{air}}] > 8\varepsilon\sigma T_{\text{leaf}}^3$. Thus megathermy can occur when air temperatures and incident solar radiation are simultaneously high.

A similar finding also occurs when stomatal conductance drops smoothly to zero:

$$\lim_{(g_S, g_S') \to 0} \beta = \frac{2\rho c_P (r_H[T_{\text{air}}] + (-T_{\text{air}} + T_{\text{leaf}}) r_H'[T_{\text{air}}]) + r_H[T_{\text{air}}]^2 (\varepsilon R_l'[T_{\text{air}}] + \alpha_s R_s'[T_{\text{air}}])}{2 r_H[T_{\text{air}}](\rho c_P + 4\varepsilon\sigma T_{\text{leaf}}^3 r_H[T_{\text{air}}])} \tag{11}$$

This equation remains complex, but under the further assumption that r_H simultaneously tends towards becoming independent of T_{air} (reasonable unless wind speed or leaf size varies with T_{air}, e.g. for species that close/move their leaves in high heat (Ehleringer and Forseth, 1980) or that evolve smaller leaves in hot and arid environments (Wright et al., 2017)), this further reduces to

$$\lim_{r_H' \to 0} \lim_{(g_S, g_S') \to 0} \beta = \frac{2\rho c_P + r_H[T_{\text{air}}](\varepsilon R_l'[T_{\text{air}}] + \alpha_s R_s'[T_{\text{air}}])}{2\rho c_P + 8\varepsilon\sigma T_{\text{leaf}}^3 r_H[T_{\text{air}}]} \tag{12}$$

In this case, the numerator exceeds the denominator when $8\varepsilon\sigma T_{\text{leaf}}^3 < \varepsilon R_l'[T_{\text{air}}] + \alpha_s R_s'[T_{\text{air}}]$. Thus megathermy can occur if there is a positive covariance between R_l or R_s and T_{air} and either convective resistance is sufficiently high or stomatal conductance is sufficiently low.

Under the alternative scenario that the stomatal conductance becomes very large and the convective resistance becomes zero,

$$\lim_{(r_H, r_H') \to 0} \lim_{g_S \to \infty} \beta = \frac{\gamma + n e_s[T_{\text{air}}] h'[T_{\text{air}}] + n h[T_{\text{air}}] e_s'[T_{\text{air}}]}{\gamma + n e_s'[T_{\text{leaf}}]} \tag{13}$$

Because e_s is a monotonic concave increasing function of T_{air}, $e_s'[T_{\text{air}}] < e_s'[T_{\text{leaf}}]$ if and only if $T_{air} < T_{leaf}$. Thus the first two terms of the numerator divided by the denominator always will be less than one if $T_{air} < T_{leaf}$, and may be less than one depending on h. Thus limited homeothermy is the likely outcome when stomatal conductance is high and convective resistance is low.

When h increases with T_{air} (i.e. warmer conditions are also relatively wetter), then the third term of Eq. (13) is positive; if this increase is sufficiently large, then the numerator of this equation can exceed the denominator, leading to $\beta > 1$ and megathermy. Alternatively if h negatively covaries with T_{air} (i.e. warmer conditions are also relatively drier), then the third term in the numerator is negative. If it becomes sufficiently negative, then the overall numerator can become negative, leading to $\beta < 0$. We are unaware of any empirical evidence for declines in T_{leaf} with increases in T_{air}, but it is a theoretical possibility.

3.3. Numerical predictions

To test our predictions for β, we also plot predictions of Eq. (4) as a function of several independent variables. Predictions are for a leaf described by the central parameter values and ranges in Table 1, with one or two parameters varying across a biologically broad range, either independently or with certain covariances with T_{air}. The central parameter values represent a medium-sized hypostomatous leaf in midday sun with light wind. To make numeric predictions, we specify the form of the saturation vapor pressure of water using the Arden-Buck equation (Buck, 1996):

$$e_S(T) = \nu_0 exp\left[\left(\frac{\nu_1 - (T - \nu_2)}{\nu_3}\right)\left(\frac{T - \nu_2}{\nu_4 + (T - \nu_2)}\right)\right] \tag{14}$$

where $\nu_1 - \nu_4$ are constants (Table 1).

To illustrate some predictions of Eq. (4), we next consider two example cases where model parameters vary with T_{air}. In the first case, we explore how variation in β arises from variation in the strengths of covariation between stomatal conductance and T_{air} [$g_S'(T_{air})$] and shortwave radiation and T_{air} [$R_s'(T_{air})$], with all other parameters set to constant central values (Fig. 2A). In this case, when covariation in either parameter is strongly positive, β can take values above or below 1, consistent with the above analysis and reflecting the contrasting influences of shortwave radiation and transpiration in heating and cooling the leaf. In the second case, we explore how predictions for β vary as a function of changes in leaf traits when non-zero covariances between stomatal conductance and T_{air} and shortwave radiation and T_{air} are incorporated (Fig. 2B). When setting $g_S'(T_{air})$ = -0.0002 m s^{-1} K^{-1} and $R_s'(T_{air})$= 30 W m^{-2} K^{-1}, and allowing the albedo α_S and the convective resistance r_H to vary, we also find that values of β can be consistent with all classes of leaf thermal response. While Fig. 2 illustrates only two of many possible examples, it demonstrates that the covariance between model parameters and T_{air} is central to influencing the realized values of β. The code provided in File S4 can be used to explore other scenarios.

3.4. An approximate solution for g_S

The above theory has highlighted the critical role of stomatal conductance in modulating T_{leaf} in different microclimates and for leaves with different traits. To better understand these tradeoffs, we also obtain an approximate solution for g_S based on energy balance theory. The full energy balance (Eq. (2)) can be algebraically re-arranged to yield

$$g_S = \frac{\gamma(2\rho c_P(T_{\text{leaf}} - T_{\text{air}}) + r_H(2\varepsilon\sigma T_{\text{leaf}}^4 - \varepsilon R_l - R_s\alpha_s))}{r_H(\gamma r_H(\varepsilon R_l - 2\varepsilon\sigma T_{\text{leaf}}^4 + R_s\alpha_s) + 2\rho c_P(\gamma T_{\text{air}} - \gamma T_{\text{leaf}} + hne_s[T_{\text{air}}] - ne_s[T_{\text{leaf}}]))} \tag{15}$$

This equation describes the value of g_S that must be obtained to balance the energy budget for a given value of T_{leaf} and T_{air}. This equation has solutions that can range from -∞ to +∞, but this full range is not physiologically relevant. We therefore next solve for the T_{leaf} values under which g_S is positive and finite.

The minimum value of g_S is zero. This value is obtained when the numerator of Eq. (15) is zero, a constraint that simplifies to

$$T_{\text{air}} = T_{leaf} - \frac{r_H}{2\rho c_P}(\varepsilon R_l + \alpha_s R_s - 2\varepsilon\sigma T_{\text{leaf}}^4) \tag{16}$$

This equation describes a curve through the T_{air}-T_{leaf} plane whose intercept decreases with increasing incident radiation and whose positive curvature and intercept increases with increasing T_{leaf}. The curve is above the 1:1 line if the outgoing blackbody radiation exceeds the incident radiation and below it otherwise.

The maximum value of g_S is +∞. This value is obtained when the denominator of Eq. (15) is zero, a constraint that simplifies to

$$\gamma r_H(\varepsilon R_l + \alpha_s R_s - 2\varepsilon\sigma T_{\text{leaf}}^4) + \rho c_P(\gamma(T_{\text{air}} - T_{\text{leaf}}) - n(e_s[T_{\text{leaf}}] - he_s[T_{\text{air}}])) = 0 \tag{17}$$

This equation can be further simplified by assuming that T_{leaf} takes a value close to T_{air}. After a first-order Taylor series expansion of T_{air} around T_{leaf}, assuming reasonably that only e_S varies with T_{leaf}, an equation can be found as:

$$T_{\text{air}} = \frac{-\gamma r_H(\varepsilon R_l - 2\varepsilon\sigma T_{\text{leaf}}^4 + R_s\alpha_s) + 2\rho c_P(-(-1 + h)ne_s[T_{\text{leaf}}] + T_{\text{leaf}}(\gamma + hne_s'[T_{\text{leaf}}]))}{2\rho c_P(\gamma + hne_s'[T_{\text{leaf}}])} \tag{18}$$

This equation now describes a unique curve in the T_{air}-T_{leaf} plane. In

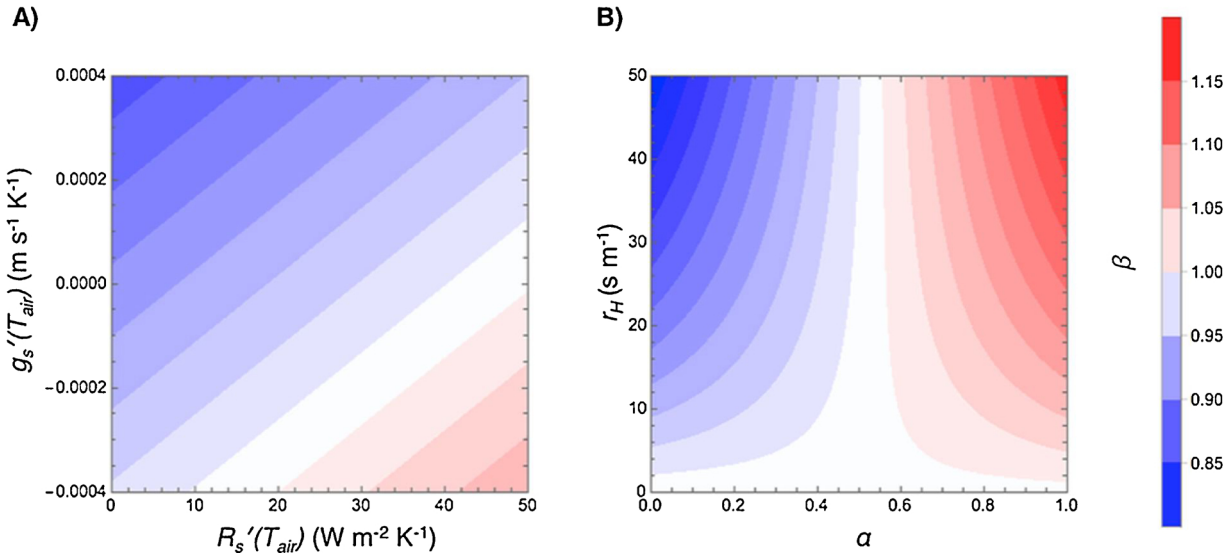


Fig. 2. Example predictions for variation in the slope β of the T_{leaf} - T_{air} relationship · Contour plots are colored redder if $\beta > 1$, gray if $\beta = 1$, and bluer if $\beta < 1$. Predictions arise from **Equation M-13** using central values in Table 1, except for the parameters that are varied in each panel. **A)** Variation in β due to changes in the strengths of covariation between T_{air} and g_S, or between T_{air} with R_s. **B)** Variation in β due to changes in the convective resistance, r_H, and the albedo, α_s, assuming covariances of $g_S'(T_{air})$ = -0.0002 m s^{-1} K^{-1} and $R_s'(T_{air})$= 30 W m^{-2} K^{-1}. (For interpretation of the references to colour in this figure legend, the reader is referred to the web version of this article).

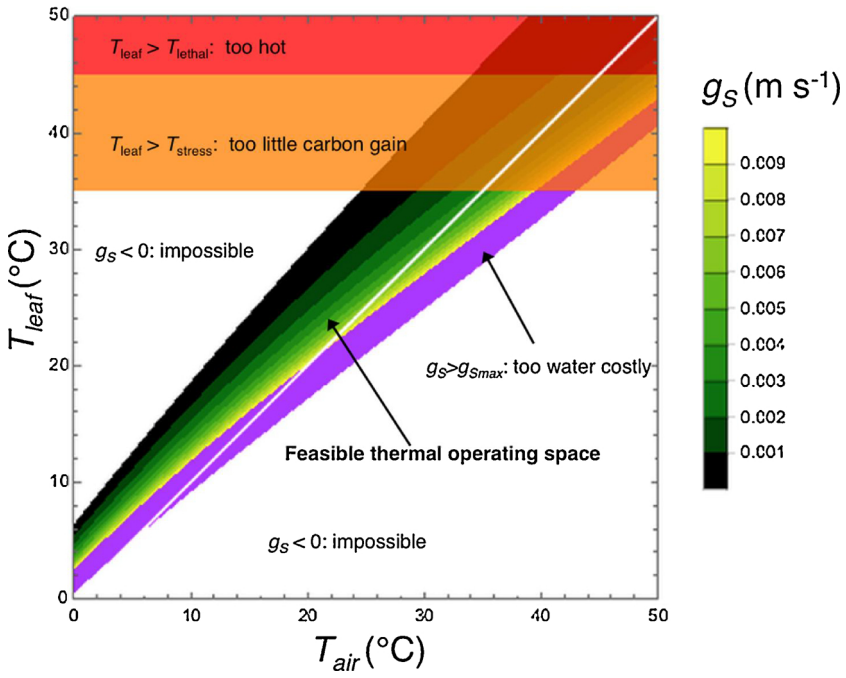


Fig. 3. Example predictions for stomatal conductance, g_S, as a function of T_{leaf} and T_{air}, with all non-focal parameters set to constant values in Table 1 except a positive covariance between air temperature and solar radiation: $R_l = R_s = 500 + 10(T_{leaf} - 273)$, corresponding to a linear increase from 500 W m^{-2} at 0 °C to 1000 W m^{-2} at 50 °C. Only a restricted range of T_{leaf} and T_{air} combinations yield a positive value of g_S (black-green-yellow shading). Values of g_S above an example physiological maximum conductance $g_{S,max}$ are shown in purple and indicate mathematically possible but physiologically impossible values. Values of T_{leaf} above a value causing stress or mortality (T_{stress} and T_{lethal}, here illustrated at 35 °C and 45 °C respectively) are shown in orange and red. The 1:1 line is shown in white. There is a restricted feasible thermal operating space corresponding to conditions not shaded in orange, red, or purple, and a limited amount of latitude for varying T_{leaf} given T_{air}. (For interpretation of the references to colour in this figure legend, the reader is referred to the web version of this article).

the case of $h = 0$, it can be interpreted as an offset from the 1:1 line where increasing radiation lowers the intercept, and increasing T_{leaf} increases the positive curvature and intercept.

The set of T_{leaf} and T_{air} values between the curves described by Eqs. (16) and (18) represents the possible thermal operating space for a leaf. However, this operating space is further constrained in two additional ways. First, the asymptote described by Eq. (18) represents $g_S = +\infty$. However, a more realistic limit would be set by a value $g_{S,max}$ that describes the physiological maximum stomatal conductance of the leaf. Such a limit would yield another curve intermediate to Eqs. (16) and (18), further restricting the thermal operating space. Additionally, there are further constraints set by $T_{leaf} < T_{stress}$ and $T_{leaf} < T_{lethal}$, where T_{stress} and T_{lethal} are temperatures at which thermal stress (often near 35 °C; Doughty and Goulden, 2008; Michaletz, 2018; Slot and Winter, 2017)

and mortality (often near 45 °C; (O'Sullivan et al., 2017)), respectively, would occur. These two additional constraints lead to a wedge-shaped band of feasible T_{air} and T_{leaf} values. To illustrate this restricted thermal operating space, we also plot numerical predictions for g_S based on Eq. (15) using the central parameter values in Table 1. The multiple constraints described above are evident in Fig. 3, leaving a narrow band of T_{air} and T_{leaf} under these operating conditions (different spaces are possible under different parameter values).

Thus, at a given value of T_{air}, the value of T_{leaf} that is actually obtained is then determined by the value of g_S that the plant sets, or the water loss rate ($E = g_S D$) that the plant is able to sustain. Or put differently, choosing a certain value of g_S at a fixed value of T_{air} leads to unavoidable changes in T_{leaf}. That is, there are unavoidable tradeoffs between water loss (E) and the risk of thermal mortality (T_{leaf}).

4. Discussion

4.1. Implications for leaf thermal response

Our main result is a conceptual clarification of the environmental and trait contexts in which each class of leaf thermal response occurs. Limited homeothermy ($\beta < 1$) is predicted when energy balance parameters are constant with respect to T_{air} (probably unrealistic) or when stomatal conductance is high and convective resistance is low (more realistic). Poikilothermy ($\beta = 1$) occurs when convective resistance is low. Megathermy can occur when microclimate or trait parameters co-vary in certain ways with T_{air}, e.g. when incident radiation or relative humidity increase with T_{air}. These results are valid under the limiting scenarios explored, but the nonlinearities in Eq. (4) also indicate that the relationships are not one-to-one. A wider range of mappings between parameters and β values are also possible (e.g. poikilothermy may also occur for other parameter combinations that do not include low convective resistance).

Our results are important for conceptually delineating when and how T_{air} is decoupled from T_{leaf}, with subsequent implications for predicting carbon/water fluxes or leaf mortality that are temperature-dependent. We showed that accounting for covariance between energy balance parameters and T_{air} is critical for accurately predicting leaf thermal response. These covariances may be set by physical or biological processes and are relevant at timescales ranging from within the lifespan of a leaf to the evolution of a clade. Our work helps identify the impact of each type of covariance on leaf thermal response. For example, within the lifespan of a leaf, if increased T_{air} leads to turgor-induced decreases in leaf angle (Fu and Ehleringer, 1989), then R_s will also decrease, leading to reductions in β. Alternatively, over evolutionary timescales, if leaf size negatively covaries with T_{air} (Ehleringer and Forseth, 1980; Wright et al., 2017), then r_H will decrease with T_{air}, and β will decrease. Additionally, environmental variables are nominally externally controlled and set the context for the leaf's thermal response, while the trait variables are nominally under the control of the organism and can modulate the leaf's thermal response, either over the lifespan of a single leaf (e.g. by varying g_S) or over ecological timescales (e.g. through trait plasticity) or over evolutionary timescales (e.g. adaptation of new phenotypes). Organisms may also indirectly modulate their microenvironment at all of these timescales by changing other traits not included in Table 1. For example, changes in branch angle or canopy openness (e.g. via changes in leaf area index) could influence R_s or r_H. Thus, many factors may allow for selection on β, or alternatively, selection on these factors may indirectly cause variation in β.

Our modeling results show that values of β can range from below 1 to above 1, whereas the majority of reported data (Dong et al., 2017; Drake et al., 2018; Michaletz et al., 2016; Yu et al., 2015) are consistent with $\beta < 1$. This mismatch requires further exploration. We suggest that because these empirical data primarily came from previously published leaf ecophysiology studies, they are biased towards observations of isolated leaves under optimal conditions for photosynthesis, i.e. the low r_H, high g_S conditions that are predicted to yield limited homeothermy. When water is limiting, stomatal conductance is low, and carbon assimilation is low (which corresponds also to realistic conditions that may not be optimal for photosynthesis, including parameter covariances with T_{air}), energy balance theory instead predicts megathermy. Some reported data have exhibited megathermy (Lin et al., 2017; Salisbury and Spomer, 1964), although such reports are few relative to those for limited homeothermy. Our original datasets (Fig. 1) are also consistent with a wide range of values of β occurring in nature. Nevertheless, they are also insufficient to formally test the predictions of our model. Comparing observed and predicted values of β would require simultaneous measurements of multiple microenvironment variables (Table 1), as in extant formal tests of extant energy budget theory. Thus, prioritizing observations of T_{leaf} in other environmental and physiological conditions and for more extreme leaf forms may lead to wider appreciation of the breadth and prevalence of thermal responses that are possible.

4.2. Implications for stomatal regulation

Our analysis of g_S in an energy balance context also highlighted the conceptual importance of thermal ecology in regulating stomatal behavior. Variation in β is likely to be critical for this coordination by either amplifying or damping changes in T_{leaf} as T_{air} varies externally. The water costs of maintaining a given leaf for a projected range of future environmental conditions probably must be traded off against the potential benefits of instead abandoning the leaf, conserving the water, and spending the water on maintaining a different leaf at a later time in different thermal environments (Sperry et al., 2016; Wolf et al., 2016). In a few limited cases, data do suggest that high transpiration can occur without photosynthesis when T_{air} is high (Drake et al., 2018; Schulze et al., 1973; Slot and Winter, 2016; Teskey et al., 2015; von Caemmerer and Evans, 2015), but it is unclear how general these results are.

We (and recently others (Drake et al., 2018)) hypothesize that in environments with high T_{air}, leaves may sometimes spend water (i.e. increase g_S, or at least decrease g_S less than predicted by classic stomatal regulation models (Medlyn et al., 2011)) in order to avoid mortality and retain the possibility of future carbon gain (Ball et al., 1988; Parkhurst and Loucks, 1972). We predict that this phenomenon would be more likely for species with costly or long-lived leaves where water is readily available, where the sunk costs or potential future carbon gain is high, or in environments where rapidly drawing down shared water resources produces a competitive advantage (Wolf et al., 2016), e.g. sun-exposed tropical forest canopies experiencing high annual precipitation (Ball et al., 1988). However, we also predict that when water is not readily available (e.g. hot deserts), g_S may not be regulated to limit high values of T_{leaf}, because conditions under which cooling would be advantageous are those where water is scarcest.

This hypothesis implies that leaves are shed when the water costs of avoiding thermal mortality exceed the carbon benefits of retaining a leaf. There is thus an opportunity to extend contemporary stomatal models which primarily focus on maximizing performance by maximizing carbon gain per unit water lost (Cowan and Farquhar, 1977), maximizing carbon profit (Sperry et al., 2016) or optimizing competition for water and avoiding hydraulic impairment (Wolf et al., 2016). These models could instead consider additional optimization criteria related to avoidance of thermal mortality, as informed by the limits identified in e.g. Fig. 3. Additionally, better data from thermally extreme environments are needed to assess whether this alternate stomatal behavior is common. Such work could improve prediction of plant water loss and carbon gain in thermally extreme environments that may become increasingly prevalent under global change (Grossiord et al., 2017; Sevanto and Xu, 2016).

Competing interests

We have no competing interests.

Author contributions

BB developed theory with input from SM. BB and SM collected data. BB and SM wrote the manuscript. SM was supported by a Los Alamos National Laboratory Director's Fellowship.

Funding

BB was supported by a UK Natural Environment Research Council independent research fellowshipNE/M019160/1. Colorado field measurements were supported by permits from the United States Forest Service and the Rocky Mountain Biological Laboratory.

Acknowledgements

Rozalia Kápás and Sabastian Escobar contributed to field measurements. Bradley Christoffersen, Charlotte Grossiord, Nate McDowell, Imma Oliveras, Nicolas Raab, Sanna Sevanto, Duncan Smith, John Sperry, Kristiina Visakorpi, and Chonggang Xu provided feedback on the manuscript.

Appendix A. Supplementary data

Supplementary data associated with this article can be found, in the online version, at https://doi.org/10.1016/j.agrformet.2018.07.012.

References

Ansari, A., Loomis, W., 1959. Leaf temperatures. Am. J. Bot. 713–717.
Ball, M., Cowan, I., Farquhar, G., 1988. Maintenance of leaf temperature and the optimisation of carbon gain in relation to water loss in a Tropical Mangrove Forest. Funct. Plant Biol. 15 (2), 263–276.
Berry, J., Bjorkman, O., 1980. Photosynthetic response and adaptation to temperature in higher plants. Annu. Rev. Plant Physiol. 31, 491–543.
Best, M.J., et al., 2011. The joint UK land environment simulator (JULES), model description – part 1: energy and water fluxes. Geosci. Model Dev. 4 (3), 677–699.
Bilger, H.-W., Schreiber, U., Lange, O., 1984. Determination of leaf heat resistance: comparative investigation of chlorophyll fluorescence changes and tissue necrosis methods. Oecologia 63 (2), 256–262.
Buck, A., 1996. Buck Research CR-1A User's Manual. Appendix 1. .
Campbell, G.S., Norman, J.M., 2012. An Introduction to Environmental Biophysics. Springer Science & Business Media.
Cowan, I.R., Farquhar, G.D., 1977. Stomatal functioning in relation to leaf metabolism and environment. In: Jennings, D.H. (Ed.), Integration of Activity in the Higher Plants. Cambridge University Press, pp. 471–505.
Dong, N., Prentice, I.C., Harrison, S.P., Song, Q.H., Zhang, Y.P., 2017. Biophysical homoeostasis of leaf temperature: a neglected process for vegetation and land-surface modelling. Glob. Ecol. Biogeogr. 26 (9), 998–1007.
Doughty, C.E., Goulden, M.L., 2008. Are tropical forests near a high temperature threshold? J. Geophys. Res. Biogeosci. 113 (G1), G00B07.
Drake, J.E., et al., 2018. Trees tolerate an extreme heatwave via sustained transpirational cooling and increased leaf thermal tolerance. Global Change Biol. 24 (6), 2390–2402.
Ehleringer, J., Forseth, I., 1980. Solar tracking by plants. Science (New York, N.Y.) 210 (4474), 1094–1098.
Fetcher, N., 1981. Leaf size and leaf temperature in tropical vines. Am. Nat. 117 (6), 1011–1014.
Fu, Q.A., Ehleringer, J.R., 1989. Heliotropic leaf movements in Common beans controlled by air temperature. Plant Physiol. 91 (3), 1162–1167.
Gates, D.M., 1964. Leaf temperature and transpiration. Agron. J. 56 (3), 273–277.
Gates, D.M., 1980. Biophysical Ecology. Courier Corporation.
Grossiord, C., et al., 2017. Tree water dynamics in a drying and warming world. Plant Cell Environ. 40 (9), 1861–1873.
Heskel, M.A., et al., 2016. Convergence in the temperature response of leaf respiration across biomes and plant functional types. Proc. Natl. Acad. Sci. 113 (14), 3832–3837.
Huey, R.B., Slatkin, M., 1976. Cost and benefits of lizard thermoregulation. Quart. Rev. Biol. 363–384.
Leuning, R., Kelliher, F.M., De Pury, D.G.G., Schulze, E.D., 1995. Leaf nitrogen, photosynthesis, conductance and transpiration: scaling from leaves to canopies. Plant Cell Environ. 18 (10), 1183–1200.
Lin, H., Chen, Y., Zhang, H., Fu, P., Fan, Z., 2017. Stronger cooling effects of transpiration and leaf physical traits of plants from a hot dry habitat than from a hot wet habitat. Funct. Ecol. 31 (12), 2202–2211.
Mahan, J.R., Upchurch, D.R., 1988. Maintenance of constant leaf temperature by plants—I. hypothesis-limited homeothermy. Environ. Exp. Bot. 28 (4), 351–357.
Medlyn, B.E., et al., 2011. Reconciling the optimal and empirical approaches to modelling stomatal conductance. Glob. Change Biol. 17 (6), 2134–2144.
Michaletz, S.T., 2018. Evaluating the kinetic basis of plant growth from organs to ecosystems. New Phytol. 219 (1), 37–44.
Michaletz, S.T., Johnson, E.A., 2006. Foliage influences forced convection heat transfer in conifer branches and buds. New phytol. 170 (1), 87–98.
Michaletz, S.T., et al., 2015. Plant thermoregulation: energetics, Trait–Environment interactions, and carbon economics. Trends Ecol. Evol. 30 (12), 714–724.
Michaletz, S.T., et al., 2016. The energetic and carbon economic origins of leaf thermoregulation. Nat. Plants 2, 16129.
Monteith, J.L., 1965. Evaporation and environment. Symp. Soc. Exp. Biol. 19, 205–234.
Monteith, J., Unsworth, M., 2007. Principles of Environmental Physics. Academic Press.
O'Sullivan, O.S., et al., 2017. Thermal limits of leaf metabolism across biomes. Glob. Change Biol. 23 (1), 209–223.
Oleson, K.W., et al., 2010. Technical Description of Version 4.0 of the Community Land Model (CLM).
Parkhurst, D.F., Loucks, O.L., 1972. Optimal leaf size in relation to environment. J. Ecol. 60 (2), 505–537.
Paw U, K.T., 1987. Mathematical analysis of the operative temperature and energy budget. J. Therm. Biol 12 (3), 227–233.
Salisbury, F.B., Spomer, G.G., 1964. Leaf temperatures of alpine plants in the field. Planta 60 (5), 497–505.
Schulze, E.D., Lange, O.L., Kappen, L., Buschbom, U., Evenari, M., 1973. Stomatal responses to changes in temperature at increasing water stress. Planta 110 (1), 29–42.
Sevanto, S., Xu, C., 2016. Towards more accurate vegetation mortality predictions. Tree Physiol. 36 (10), 1191–1195.
Sitch, S., et al., 2003. Evaluation of ecosystem dynamics, plant geography and terrestrial carbon cycling in the LPJ dynamic global vegetation model. Glob. Change Biol. 9 (2), 161–185.
Slot, M., Winter, K., 2016. The effects of rising temperature on the ecophysiology of tropical forest trees. In: Goldstein, G., Santiago, L.S. (Eds.), Tropical Tree Physiology. Springer.
Slot, M., Winter, K., 2017. In situ temperature response of photosynthesis of 42 tree and liana species in the canopy of two Panamanian lowland tropical forests with contrasting rainfall regimes. New Phytol. 214 (3), 1103–1117.
Smith, W., 1978. Temperatures of desert plants: another perspective on the adaptability of leaf size. Science (New York, N.Y.) 201 (4356), 614–616.
Smith, W.K., Carter, G.A., 1988. Shoot structural effects on needle temperatures and photosynthesis in conifers. Am. J. Bot. 75 (4), 496–500.
Sperry, J.S., et al., 2016. Predicting stomatal responses to the environment from the optimization of photosynthetic gain and hydraulic cost. Plant Cell Eviron. 40 (6), 816–830.
Teskey, R., et al., 2015. Responses of tree species to heat waves and extreme heat events. Plant Cell Environ. 38 (9), 1699–1712.
Tuzet, A., Perrier, A., Leuning, R., 2003. A coupled model of stomatal conductance, photosynthesis and transpiration. Plant Cell Environ. 26 (7), 1097–1116.
von Caemmerer, S., Evans, J.R., 2015. Temperature responses of mesophyll conductance differ greatly between species. Plant Cell Environ. 38 (4), 629–637.
Wolf, A., Anderegg, W.R.L., Pacala, S.W., 2016. Optimal stomatal behavior with competition for water and risk of hydraulic impairment. Proc. Natl. Acad. Sci. 113 (46), E7222–E7230.
Wright, I.J., et al., 2017. Global climatic drivers of leaf size. Science (New York, N.Y.) 357 (6354), 917–921.
Yu, M.H., et al., 2015. How the plant temperature links to the air temperature in the desert plant Artemisia ordosica. PloS One 10 (8), e0135452.